DNA Polyintercalating Drugs. Proton Magnetic Resonance Studies of a New Acridine Dimer. Conformations and Interactions with Mono- and Dinucleotides†

Jacques Barbet, Bernard P. Roques,* Suzanne Combrisson,‡ and Jean Bernard Le Pecq§

ABSTRACT: The conformation in aqueous solution of one acridine dimer which is able to bisintercalate in DNA (1,14-bis(2-methoxy-6-chloro-9-acridinyl)-1,5,10,14-tetraazatetradecane tetrahydrochloride) (AcDi) and its interactions with mono- and dinucleotides have been investigated by fast Fourier transform proton magnetic resonance spectroscopy. Variations in chemical shifts of the most distinguishable protons of the acridine dimer with temperature bring evidence of a folded ⇌ unfolded fast conformational equilibrium in the temperature range of 4–85 °C. Equilibrium parameters were estimated. The folded conformation has been deduced from iso-shielding curves of the acridine ring. In the complex between AcDi and 3′- or 5′-AMP, the adenine ring is intercalated between the two acridine rings to give a sandwich-like complex. Studies of interaction with adenylyl(3′→5′)adenosine (ApA) show two different complexes in equilibrium with the 3′ or the 5′ moiety of ApA intercalated in the acridine dimer. These conclusions are derived from comparative studies with 2-methoxy-6-chloro-9-(3-dimethylaminopropylamino)acridine dihydrochloride which is the corresponding acridine monomer (AcMo). In that case the self-association constant was determined. A model of the AcMo–5′-AMP complex was deduced from the analysis of the chemical shifts of the adenine protons. In this model, the N_{10}^{+}–D bond of the acridine points toward the negatively charged phosphate of the nucleotide.

Many studies have shown that a great number of drugs and antibiotics bind to DNA in vitro with a high affinity according to the intercalation model first described by Lerman (1961) and recently confirmed by x-ray diffraction analysis (Tsai et al., 1975). The most extensively studied drugs are either antitumoral compounds, actinomycin D (Müller and Crothers, 1968) and ellipticine derivatives (Le Pecq et al., 1975), or antiparasitic drugs, aminoacridine (Lerman, 1963, 1964) and ethidium bromide (Waring, 1965; Le Pecq and Paoletti, 1967). It has been generally admitted that the biological activities of these compounds are related to their reactivity with DNA. It is therefore logical in a search for such drugs to design molecules which have the highest possible affinity for DNA. Affinities of the order of 10^{10} to 10^{12} M^{-1}, comparable to that of RNA polymerase or repressor, can simply be obtained using polymers, because binding constant increases rapidly with the number of subunits. Along this line we have chosen to synthesize and study polymers made up of intercalating units. Our first approach was to synthesize acridine dimers (Barbet et al., 1975). As expected some of the compounds which bis-intercalate in DNA have binding constants ($>10^{8}$ M^{-1}) very much larger than that of the monomeric unit (10^{5} M^{-1}, Le Pecq et al., 1975). On the other hand, such compounds might possess properties depending on the DNA sequence (Le Pecq et al., 1975). In order to understand these properties, information on the conformation of the chain linking the subunits and on the geometry of the intercalated complexes is of special importance. The studies of Jain and Sobell (1972), Krugh and Neely (1973), Krugh et al. (1975), and Patel (1972) have shown that these later problems can be validly approached by studying the interaction of the intercalating molecules with mono- and dinucleotides. Valuable information has been obtained in the solid state by crystallographic studies (Jain and Sobell, 1972; Tsai et al., 1975; Seeman et al., 1975; Courseilles et al., 1976). In solution, proton magnetic resonance (^{1}H NMR), thanks to its extreme sensitivity to conformational changes within molecules and to environment, is particularly useful for the study of such problems (Jardetzky and Jardetzky, 1960; Schweitzer et al., 1965; Kreishman et al., 1971; Patel, 1972; Krugh et al., 1975). Because of the very low solubility of acridine dimers, such studies must be performed by fast Fourier transform nuclear magnetic resonance. This method allows investigations at relatively low concentrations (10^{-2} to 10^{-4} M) which are close to the concentrations at which the molecules elicit biological properties. In this paper, we report ^{1}H NMR studies on the conformations of an acridine dimer able to bis-intercalate in DNA (Le Pecq et al., 1975): 1,14-bis(2-methoxy-6-chloro-9-acridinyl)-1,5,10,14-tetraazatetradecane tetrahydrochloride (AcDi) in aqueous solution. Its interactions with 3′- and 5′-AMP and with the dinucleotide ApA have been compared with that of an acridine monomer (AcMo; 2-methoxy-6-chloro-9-(3-dimethylaminopropylamino)acridine dihydrochloride); see Figure 1.

Materials and Methods

Materials. 5′-AMP[1] was purchased from Calbiochem, San Diego, Calif., 3′-AMP from Schwarz Bioresearch Inc., Mount Vernon, N.Y., and ApA from Aldrich Chemical Company

† From the Département de chimie, Ecole Polytechnique, 75230 Paris Cedex 05, France. *Received August 4, 1975.* This work was presented in the VIth International Conference on Magnetic Resonance in Biological Systems, Kandersteg, Switzerland, September 16–21, 1974. This investigation was supported by the Centre National de la Recherche Scientifique, France (ATP Pharmacodynamie et Chimiothérapie) and by the Fondation de la Recherche Médicale Française.

‡ Present address: Laboratoire de Recherches organiques, ESPCI, 75005 Paris, France.

§ Present address: Laboratoire de Pharmacologie moléculaire associé au CNRS No. 147 Institut Gustave-Roussy, 94800 Villejuif, France.

[1] Abbreviations used: AcDi, acridine dimer; AcMo, acridine monomer; 5′-AMP, adenosine 5′-monophosphate; 3′-AMP, adenosine 3′-monophosphate; ApA, adenylyl(3′→5′)adenosine; exp, experimental; th, theoretical.

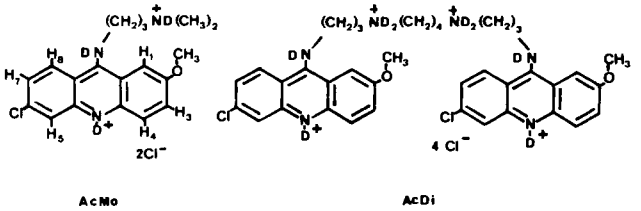

FIGURE 1: Chemical structure of the acridine monomer and dimer used in this work.

Inc., Milwaukee, Wis.; these were used without further purification. Acridine monomer and dimer (structure shown in Figure 1) were synthesized and purified in the laboratory as previously described (Barbet et al., 1975).

Instrumentation. ^{1}H NMR spectra were recorded at 100 MHz with a Varian Associate XL-100-12 spectrometer operating on the Fourier transform mode. Probe temperatures were regulated by a Varian Associate temperature controller and monitored by observing the splitting in ethylene glycol. This spectrometer was locked to the deuterium resonance of solvent (D_2O). Chemical shifts were measured from an external hexamethyldisiloxane in CCl_4 reference and reliable to ± 0.01 ppm.

Variable-temperature ^{1}H NMR spectra were also recorded at 250 MHz with a Cameca-250 spectrometer operating on the Fourier transform mode. The same techniques were employed but the locking of the spectrometer was unnecessary.

Extrapolated values to infinite dilution were estimated with an accuracy of about 0.02 ppm.

Procedures. Except for the double-resonance ^{1}H NMR experiments, the spectra were recorded with a strong and continuous irradiation of the HOD solvent resonance in order to reduce its intensity. The HOD signal intensity was then reduced by a factor of about 40.

Solutions were made either in pure D_2O or in a buffer containing 0.1 mol of acetic-d_4 acid adjusted to the desired value of pD with NaOD. The apparent pD values in D_2O solvent were determined with a Tacussel TS 60/N pH meter according to the equation, pD = meter reading + 0.4 (Glasoe and Long, 1960). The concentrations of the stock solutions were measured by spectrophotometric analysis.

When it was necessary, chemical shifts of aromatic protons were determined from simulated spectra run on a Benson plotter connected to a UNIVAC-1108 computer, using a Lorentzian line profile.

Results and Discussion

(1) *Spectrum and Assignment of the Acridine Monomer.* According to our knowledge, proton resonances of quinacrine-like molecules in aqueous solutions have not yet been assigned. The 100-MHz ^{1}H NMR spectrum of a diluted solution (4.5×10^{-3} M, 48 °C) of AcMo in D_2O shows two ABC systems in the aromatic region without any interring coupling constant (Figure 2). Thanks to double-resonance ^{1}H NMR, the resonances of each ABC system are easily distinguished, but it is more difficult to know which is the ABC system corresponding to the methoxy or the chlorine substituted ring. So, in a first step, it was necessary to ascertain the assignment of one peculiar resonance. When the methoxy group of AcMo in a carefully degassed solution is irradiated, the doublet at 7.69 ppm exhibits a significant increase ($\simeq$20%) which may result either from a nuclear Overhauser effect or from suppression of long-range coupling constants between OCH_3 and H_1 or H_3 (Figure 3B). Whatever the cause of this phenomenon, it can be concluded that the doublet at 7.69 ppm contains the H_1 or H_3 resonances. Furthermore if the spectrum of AcMo is recorded with 90° pulses and a 2-s acquisition time without delay, the doublet ($J \simeq 2$ Hz) at 7.83 ppm disappears almost completely (Figure 3C). We can assign this signal to H_5 because this proton is expected to have the longest T_1 in the molecule (no proton in its vicinity).

Finally the irradiation of the quartet at 7.54 ppm causes the collapse of the 2-Hz meta coupling constant of H_5 and of the 9.5-Hz ortho coupling constant of the low-field doublet (Figure 3D). Thus the multiplet centered at 7.69 ppm contains H_1, H_3, and H_4. The H_8 resonance is at 8.31 ppm, H_5 at 7.83 ppm, and H_7 at 7.54 ppm.

We find H_8 downfield shifted from the other aromatic protons in several solvents (water, dimethyl sulfoxide, methanol) either in the basic or protonated form, but not in chloroform. Such a behavior may result from a peculiar orientation of the side chain which permits a specific solvation of the 9-NH group bringing the bound solvent in the vicinity of H_8. In

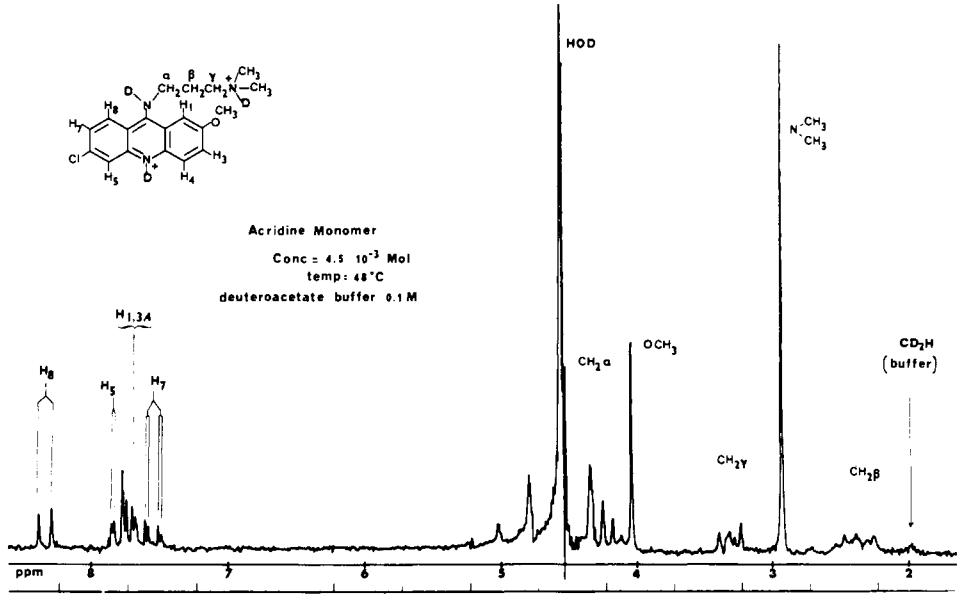

FIGURE 2: Spectrum of the acridine monomer.

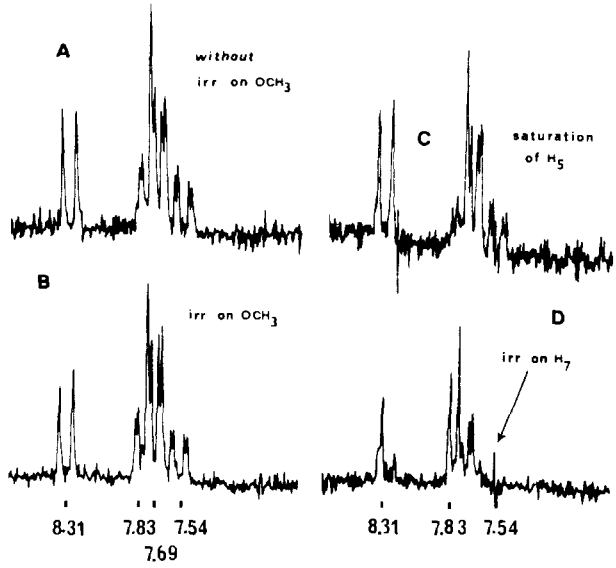

FIGURE 3: Assignment of the aromatic protons of the acridine monomer.

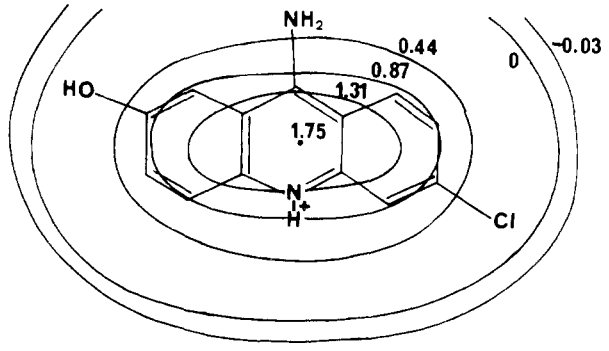

FIGURE 4: Ring-current map for 2-hydroxy-6-chloro-9-aminoacridine.

agreement with this view point, x-ray studies have shown that the side chain in a closely related compound is lying roughly in the plane of the molecule with the terminal $NH((CH_2)_2OH)_2$ group bending toward the OCH_3 (Carrel, 1972).

(2) Estimation of the Geometry of Complexes Using the Ring-Current Map of 2-Hydroxy-6-chloro-9-aminoacridine. Giessner Prettre and Pullman (personal communication) have evaluated the ring-current shifts in a plane parallel and 3.4 Å from the acridine ring (Figure 4). Thanks to this map we were able to compute theoretical upfield shift values for all protons of a molecule stacked with this acridine in any position. Taking into account steric restrictions and electrostatic repulsions, the geometry which gave the best fit between calculated and observed values of the chemical shifts was retained.

(3) Study of Acridine Monomer Self-Association. This type of molecule is known to stack extensively in aqueous solution (Chan et al., 1964; Blears and Danyluk, 1967; Thomas and Roques, 1972). Thus, vertical stacking of the aromatic heterocycles is also probable in that case. In order to estimate the magnitude of this phenomenon, we studied the concentration dependence of the proton chemical shifts of AcMo. We recorded at 21 °C the spectra from 4.5×10^{-4} up to 3.64×10^{-2} M (Figure 5). This last concentration corresponds to an almost saturated solution. The chemical shifts are plotted against concentration and extrapolated at infinite dilution (Figure 6). Obviously errors must be small to calculate for each concentration and for each proton $\delta\sigma$ (difference between extrapolated

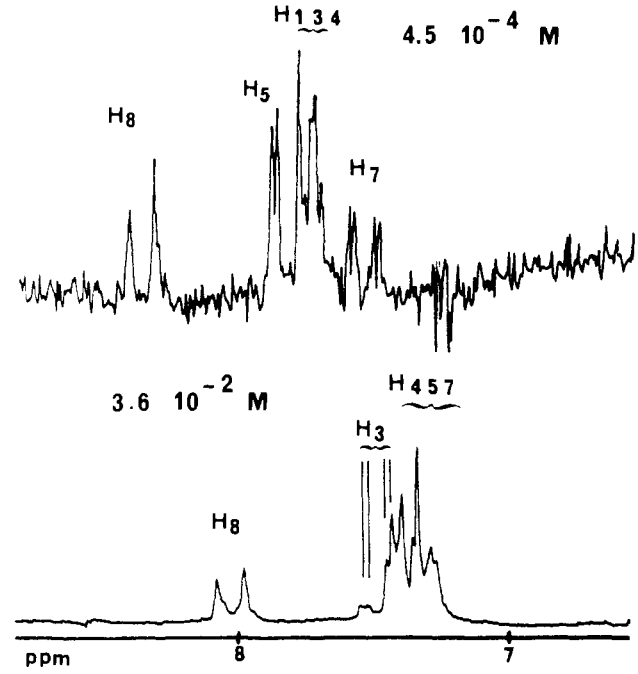

FIGURE 5: Concentration dependence of the spectra of the acridine monomer (aromatic part).

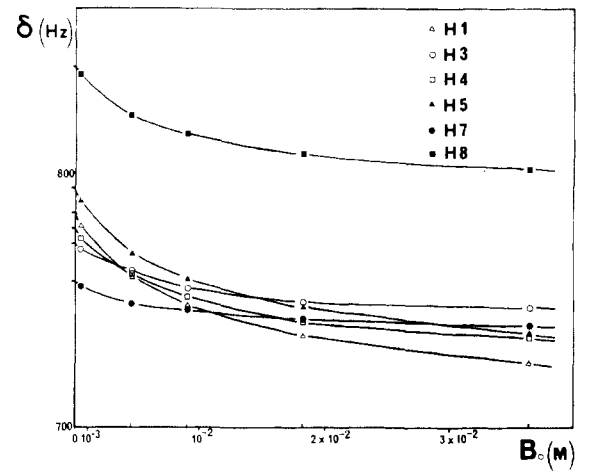

FIGURE 6: Concentration dependence of the chemical shifts (δ in Hz from hexamethyldisiloxane, external reference) of the acridine monomer protons at 21 °C, pD 6.3. The chemical shifts were determined by comparison of simulated and experimental spectra.

chemical shift at infinite dilution and actual chemical shift at a given concentration). Assuming that AcMo self-associates to form vertically stacked *n*-mers we can use the equations of Dimicoli and Hélène (1973). The association constant (K) and the difference of chemical shifts of every proton between free molecule and stacked dimer ($\delta\sigma B_2$) are determined. Let us recall the hypotheses made for this calculation: (i) successive association constants are identical; (ii) effects of magnetic anisotropy are additive; (iii) only the magnetic anisotropy of the nearest neighbors is taken into account.

Let B_0 be the total concentration of AcMo. A plot of $(\delta\sigma/B_0)^{1/2}$ vs. $\delta\sigma$ gives a straight line of which slope (s) and x-axis intercept (x_0) are respectively $(K/2\delta\sigma B_2)^{1/2}$ and $(2\delta\sigma B_2)$ (Figure 7). Therefore $\delta\sigma B_2$ is directly obtained from these plots and the association constant K is calculated ($K = x_0 s^2$) for each proton. The same experiment was also performed at 48 °C in the presence of deuterated acetate buffer (0.1 M, pD

Table I: Self-Association Induced Chemical Shifts and Self-Association Constants for AcMo in D_2O (21 °C) and Deuterioacetate Buffer (0.1 M; pD 5.5, 48 °C).

	21 °C			48 °C		
Proton	$\delta\sigma B_{2exp}$ (ppm)	$\delta\sigma B_{2th}$ (ppm)	K (M^{-1})	$\delta\sigma B_{2exp}$ (ppm)	$\delta\sigma B_{2th}$ (ppm)	K (M^{-1})
H_1	0.48	0.46	100	0.28[a]	0.46	78
H_3	0.22	0.30	103	0.28[a]	0.30	78
H_4	0.35	0.33	108	0.28[a]	0.33	78
H_5	0.47	0.46	108	0.38	0.46	79
H_7	0.14	0.28	109	0.16	0.28	70
H_8	0.34	0.33	112	0.29	0.33	78
OCH_3	0.08			0.07		
$N(CH_3)_2$	−0.02			−0.01		
$CH_2\alpha$	0.19		111	0.16		
$CH_2\beta$	0.04			0.05		
$CH_2\gamma$	−0.02			0.02		
Av values:			107			76

[a] Unresolved multiplet.

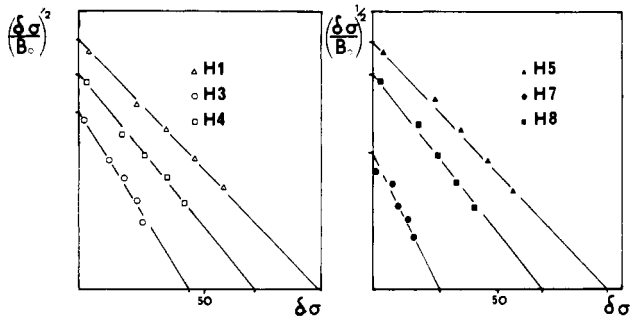

FIGURE 7: Self-association of acridine monomer in D_2O at 21 °C, pD 6.3. B_0 is the total concentration of AcMo; $\delta\sigma$ is the difference between extrapolated chemical shift at infinite dilution and actual chemical shift at a given concentration. The x-axis intercept equals $2\delta\sigma B_2$ and the slope is $(K/2\delta\sigma B_2)^{1/2}$, K being the self-association constant and $\delta\sigma B_2$ the difference in chemical shift between the stacked dimer and the monomer.

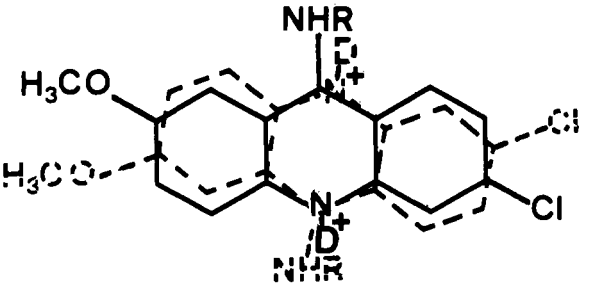

FIGURE 8: Model for the self-association of the acridine monomer.

5.5). The results are similar but the association constant is somewhat lower (Table I).

It is clear, from the results shown in Table I, that the different protons of the acridine ring are not affected in the same way by the aggregation. By systematic comparison of experimentally determined $\delta\sigma B_{2exp}$ and $\delta\sigma B_{2th}$ deduced from iso-shielding curves, as discussed above (section 2), a tentative model of the association between two molecules of AcMo at 21 °C can be proposed. It is assumed that the side chains have to be kept far from each other in order to minimize their repulsive electrostatic interactions. Therefore the configuration with one chromophore inverted with respect to the other is preferred as in the self-association of many other intercalating dyes (ethidium, Thomas and Roques, 1972; actinomycin, Angerman et al., 1972). The geometry of the complex (Figure 8) can be supported by the following arguments: (i) The large difference between the $\delta\sigma B_{2exp}$ of H_4 and H_5 excludes a perfectly superimposed stacking. (ii) If the methoxy group of one molecule and the chlorine atom of the other are put on the same side of the stack, the environments of H_5, for instance, in the two molecules are not identical and the shielding experienced by this proton is averaged. Therefore such a model which predicts very similar $\delta\sigma B_{2th}$ for H_5 and H_8 is very unlikely. (iii) If the angle between the two long axes of the stacked molecule is set at 90°, H_3 and H_7 fall in a nonshielding area. The importance of the shielding of these protons (0.22 and 0.17 ppm) rules out this possibility. Of course the proposed model is approximate because the extrapolated experimental values and the computed iso-shielding curves have limited accuracies.

If it is assumed that AcMo can only form stacked dimers, a plot of $(\delta\sigma/B_0)^{1/2}$ vs. $\delta\sigma$ would give also a straight line, but x_0 would then be $\delta\sigma B_2$ and agreement is no longer found with the calculated values. Consequently this favors the formation of n-mers.

(4) Acridine Dimer Conformation. The low solubility of AcDi prevented us from studying its intermolecular stacking. Nevertheless, AcDi, as well as AcMo, probably forms aggregates when the concentration is increased. But there are striking differences between the spectra of AcMo and AcDi, even at very low concentration (4.5×10^{-4} M, 21 °C) in conditions where it is reasonable to assume that intermolecular stacking may be neglected (less than 4% of stacked molecules). Inductive effect of side chains cannot be the cause of such differences. The large upfield shifts of the protons in AcDi as compared with AcMo can be interpreted by the formation of an intramolecular stacked complex.

Increasing temperature must destabilize a folded conformation and at high temperature the spectra of AcDi must become similar to that of AcMo (Chan and Nelson, 1969). Therefore the temperature dependence of the chemical shifts of the protons of AcDi and AcMo for the same concentration of acridine moieties (3.6×10^{-3} M) was measured from 4 to 85 °C (Figure 9). The plots of the relative chemical shifts $\delta\sigma_s$ vs. temperature show the characteristic shape of a "melting" curve (Figure 10A). This confirms the existence in solution of a folded conformation in equilibrium with an unfolded one. The

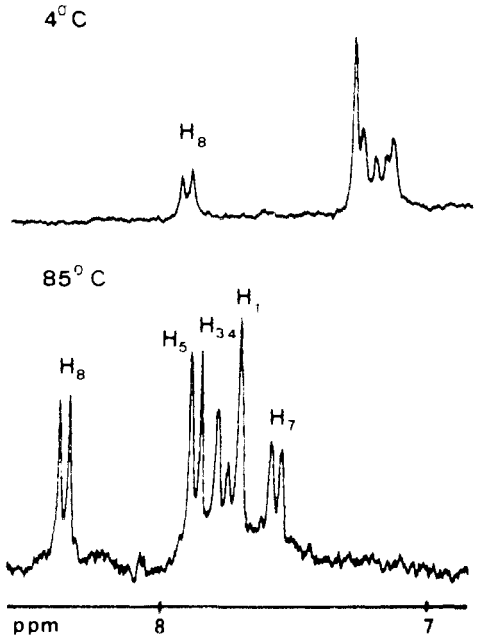

FIGURE 9: Temperature dependence of the spectra of the acridine dimer (250 MHz).

equilibrium constant can be easily evaluated at each temperature through the relation

$$K_s = \frac{\delta\sigma_s - \delta\sigma_{sr}}{\Delta\sigma_s}$$

with $\delta\sigma_{sr}$ being the residual chemical-shift difference between AcMo and AcDi at high temperature where no folded form is present and $\Delta\sigma_s$ the chemical-shift difference between completely folded and unfolded forms of AcDi. The residual term $\delta\sigma_{sr}$ may be due to inductive effects of side chains. For all protons this term is weak (<0.08 ppm). $\Delta\sigma_s$ is difficult to evaluate by extrapolation because, even at 4 °C, AcDi is not completely folded. However, a plot of ln K_s against $1/RT$ gives a straight line only when $\Delta\sigma_s$ is correctly evaluated; from these results (Figure 10B), the thermodynamic parameters evaluated for each proton are strikingly close ($\Delta H_0 = -8.0$ kcal/mol, $\Delta s_0 = -27.5$ eu; melting temperature, 15 °C). These values are similar to those determined for the intramolecular stacking of ApA (Brahms et al., 1966; Brahms and Van Holde, 1967) and NAD (McDonald et al., 1972). A model for this intramolecular stacking based on considerations of magnetic anisotropy can be proposed. This model is consistent with the specific shieldings $\Delta\sigma_s$ of the various acridine protons (Table II) and with the steric restrictions estimated from the examination of space filling molecular model (Figure 11). The agreement between observed and calculated $\Delta\sigma_s$ supports the accuracy of evaluated thermodynamic parameters. This folded conformation (Figure 11) brings in close proximity the two protonated ring nitrogens: this could explain why acridine dimers like AcDi have pK_a's significantly lower (≤ 7; our measurements) than quinacrine (7.92) and AcMo (8.01) (Irvin and Irvin, 1950).

In a 0.1 M acetate buffer this temperature dependence of the equilibrium is no longer observed. The melting temperature seems to be increased to about 100 °C. This behavior can be understood in terms of the screening of positive charges in the aggregate through the attraction of negative charges from the surrounding medium (Robinson et al., 1973). Therefore in the following experiments in acetate buffer we can assume that AcDi is almost completely folded.

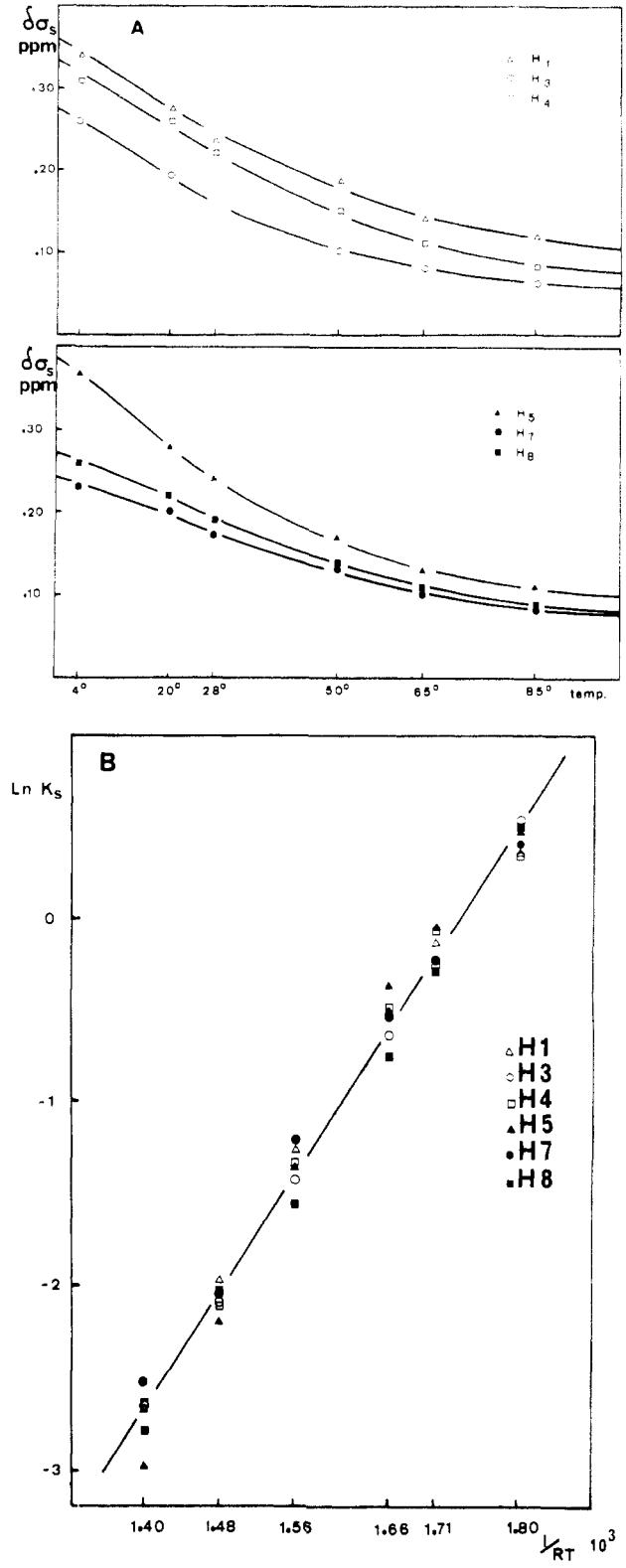

FIGURE 10: (A) Relative chemical shifts ($\delta\sigma_s$) between AcMo and AcDi as a function of temperature. (Chemical shifts were determined as in Figure 6.) (B) Plots of ln K_s vs. $1/RT$, for the folded-unfolded equilibrium of AcDi.

(5) Acridine Monomer–5′-AMP Interaction. In order to facilitate the study of the interaction of acridine dimer with nucleotides, we have first studied the interaction of AcMo and 5′-AMP in deuterioacetate buffer, 0.1 M (3.5×10^{-3} M, pD 5.5, 25 °C and 3×10^{-3} M, pD 5.5, 48 °C), by analysis of mixing curves according to the method of continuous variations

Table II: Conformation of the Acridine Dimer. Observed and Evaluated Shielding ($\Delta\sigma_s$).

Protons	H_1	H_3	H_4	H_5	H_7	H_8
Observed $\Delta\sigma_s$ (ppm)	0.43	0.35	0.38	0.46	0.29	0.32
Evaluated $\Delta\sigma_s$[a] (ppm)	0.44	0.34	0.43	0.46	0.29	0.33

[a] Evaluated from iso-shielding curves with the two acridine rings at 3.4 Å according to the model of Figure 9.

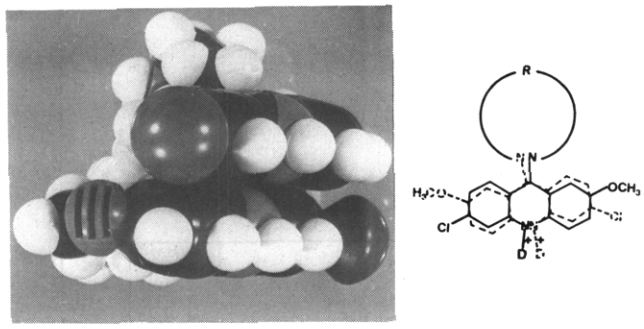

FIGURE 11: Molecular model for the folded conformation of the acridine dimer.

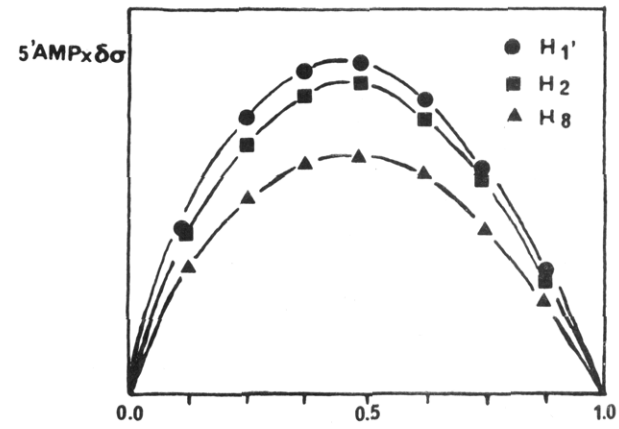

FIGURE 12: Job plot for the interaction between acridine monomer and 5′-AMP. r = concentration of AcMo with AcMo + 5′-AMP (concentration of AcMo plus concentration of 5′-AMP) kept constant. (3.5×10^{-3} M). Measurements are done at pD 5.5 and 25 °C.

(Job, 1928).

Let $\delta\sigma_c$ be the chemical-shift difference between the protons of 5′-AMP and 5′-AMP in the mixture 5′-AMP–AcMo. If the sum of the concentrations of the two compounds ([5′-AMP] + [AcMo]) is kept constant and the ratio [AcMo]/[5′-AMP] is varied, the variations of [5′-AMP] $\times$ $\delta\sigma_c$ vs. r = [AcMo]/([5′-AMP] + [AcMo]) (Figure 12) give an usual Job plot.

In the range of the concentration used here, it can be assumed that 5′-AMP is completely unstacked while about 30% of acridines are still associated. The Job plots obtained indicate that the stoichiometry of the complex is near 1:1. The slight dissymmetry of the curves may be due to the stronger stacking of AcMo molecules at high r values or to the presence of some 2:1 5′-AMP–AcMo complex. The extrapolated induced chemical shifts $\delta\sigma_{cex}$ at $r = 1$, [5′-AMP] = 0, indicate an almost similar effect on the three protons at each temperature. These extrapolated shifts ($\delta\sigma_{cex}$) in this method are equal to:

$$\frac{K_c B_0}{1 + K_c B_0} \Delta\sigma_c$$

K_c being the association constant, B_0 the total concentration ([5′-AMP] + [AcMo]), and $\Delta\sigma_c$ the chemical shift induced by total complexation. Therefore these extrapolated values are directly related to the effect of the acridine magnetic anisotropy on 5′-AMP.

In the method of continuous variations, when r decreases, the self-association of AcMo falls, while the co-staking with 5′-AMP increases. So the resulting chemical-shift changes of the protons of the acridine derivatives have no simple significance. However, we noticed that the induced chemical shifts on the acridine protons are very small.

We attempted to measure the AcMo–5′-AMP interaction constant at 48 °C in deuterated acetate buffer solution ([5′-AMP] = 3×10^{-3} M, pD 5.5) by varying the concentration of AcMo from 10^{-2} to 3×10^{-2} M according to Dimicoli and Hélène (1973). Because of the small concentration range used in the measurement, the determined interaction constant ($\simeq$70 M^{-1}) is quite inaccurate, but nevertheless one can say that this constant is of the same order of magnitude as the self-association constant of AcMo. At 48 °C we found that the extrapolated chemical shifts for $r = 1$ dramatically decreased compared with those obtained at 25 °C. In these conditions with $B_0 = 3 \times 10^{-3}$ M and $K_c = 70$ M^{-1}, the factor $K_c B_0/(1 + K_c B_0)$ is nearly equal to 0.17. Then we can calculate $\Delta\sigma_c$: the chemicals shifts of the H_2, H_8, and $H_{1'}$, protons of 5′-AMP induced by total complexation

$$\Delta\sigma_c = \Delta\sigma_{cex} \frac{1 + K_c B_0}{K_c B_0}$$

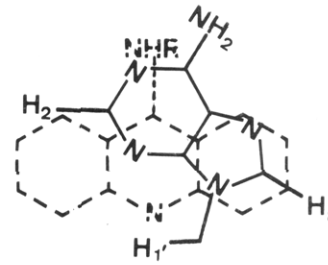

FIGURE 13: Stacking geometry of the complex between acridine monomer and 5′-AMP.

In 5′-AMP molecule, the three protons H_2, H_8, and $H_{1'}$ lie in the plane of the adenine ring and are far from each other. Taking into account the rough similarity of the induced chemical shifts, $\Delta\sigma_c$, and the steric hindrance due to the lateral chain of AcMo and to the ribose moiety of 5′-AMP, we are able to propose a preferential geometry for which agreement between $\Delta\sigma_c$ and $\Delta\sigma_{th}$, evaluated from ring current calculations, is satisfactory. Under these conditions it is possible to find a model consistent with the sequence $\Delta\sigma_c H_{1'} > \Delta\sigma_c H_2 > \Delta\sigma_c H_8$. In this model, the N_{10}^+–D bond of the intracyclic nitrogen is directed toward the negatively charged phosphate (Figure 13). With the $\Delta\sigma_{cth}$ values calculated from ring current shifts, it is possible to have an estimation of K_c at 25 °C ($K_c \simeq 215$ M^{-1}). All these results are reported in Table III.

(6) Acridine Dimer–AMP Interactions. At room tempera-

Table III: Extrapolated ($\delta\sigma_{cex}$), Calculated ($\Delta\sigma_c$), and Evaluated ($\Delta\sigma_{cth}$) Chemical Shifts for 5′-AMP Protons in the Acridine Monomer–5′-AMP Complex (Deuterioacetate Buffer, 0.1 M, pD 5.5).

Proton	$\delta\sigma_{cex}$, $B_0 = 3.5 \times 10^{-3}$ M, 25 °C, Ac Buffer (0.1 M)	$\delta\sigma_{cex}$, $B_0 = 3 \times 10^{-3}$ M, 48 °C, Ac Buffer (0.1 M)	$\Delta\sigma_c$ Calcd from K_c and $\delta\sigma_{cex}$, 48 °C	$\Delta\sigma_{cth}$[a]
H_1	0.29	0.11	0.64	0.66
H_2	0.27	0.10	0.59	0.63
H_8	0.22	0.09	0.53	0.53

[a] Evaluated from iso-shielding curves with the acridine and the 5′-AMP rings at 3.4 Å from each other according to the model of Figure 13.

ture, a 2.4×10^{-3} M solution of AcDi and 3′- or 5′-AMP (pD 5.5) gives a precipitate which can be recovered from the supernatant by centrifugation and dissolved in Me_2SO-d_6. The ^1H NMR analysis of the solution shows that the precipitate contained an equimolar mixture of AcDi and AMP. Under these conditions, high molecular weight aggregates are formed and the interaction between AcDi and AMP cannot be studied. Such inconvenience can be avoided by making the measurement at a lower pD or at higher temperature. At pD 3 no interaction is observed. The spectrum of the mixture is the exact superposition of the spectra of the constituents. At such pD, the adenine ring is protonated and this prevents the interaction owing to electronic repulsions.

At 48 °C, the mixture of the two solutions stayed limpid and an important interaction is still observed. So we have chosen to study the interactions between nucleotides and acridine dimer at 48 °C in a deuterated acetate buffer (pD 5.5).

The mixing curves for AcDi–3′-AMP are symmetrical but not for AcDi–5′-AMP, indicating a 1:1 complex for 3′-AMP and a mixture of 1:2 and 1:1 complexes for 5′-AMP (Figure 14). It is interesting to note that the induced chemical shifts extrapolated for [AMP] = 0 are equal to

$$\frac{K_c B_0}{1 + K_c B_0} \Delta\sigma_c$$

$\Delta\sigma_c$ being the difference between the 1:1 complex and free AMP chemical shifts even when a 1:2 complex is present. The extrapolated values $\delta\sigma_{cex}$ for the complexes between 3′- and 5′-AMP with AcDi (Table IV) can be compared, even if the uncertainty is relatively large (≤10%). Indeed in 5′-AMP–AcDi complex, H_1' is a little more affected than H_2, the difference being obviously in the error range; in the 3′-AMP–AcDi complex, H_2 is more affected than H_1' and in this case the difference (0.11 ppm) is clearly larger than the experimental error. Thus it is reasonable to conclude that the adenine ring and the dimer adopt a preferential orientation and that these geometries of the complexes are governed by the esterification site of the phosphate. On the other hand the value of observed shifts (between 0.23 and 0.40 ppm) is far more important in this case than with the monomer (0.09–0.11; Table III). To explain this enhancement we have to suppose an increase of either the association constant K_c or of the differences $\Delta\sigma_c$. If we observe the proton shifts of the dimer we notice that, when AcDi concentration decreases ($r \rightarrow 0$), a slight deshielding is observed and the spectrum aspects (relative positions of the peaks) are getting more and more similar to those

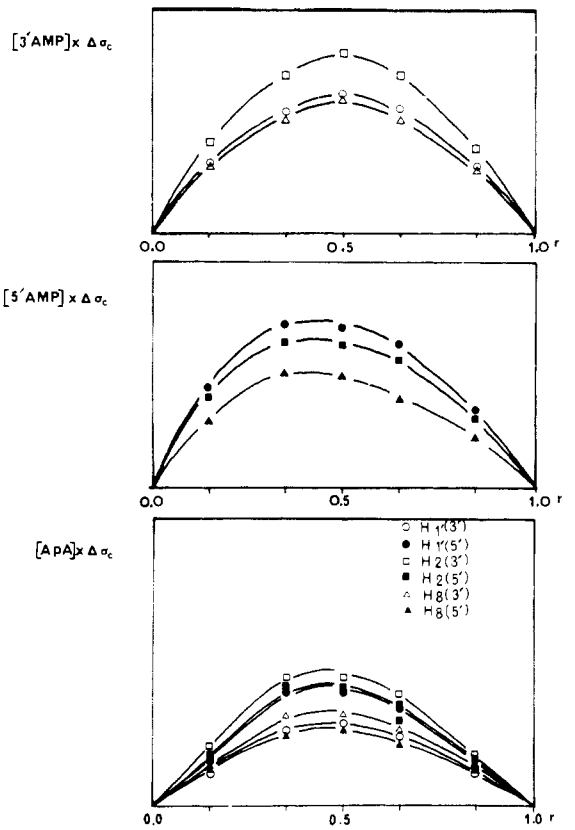

FIGURE 14: Job plots for the interactions between acridine dimer with 3′-AMP, 5′-AMP, and ApA. r is the same as in Figure 12. Total concentration of reactants is 2.4×10^{-3} M. Measurements are done at pD 5.5 and 48 °C.

of the totally unfolded product obtained at 85 °C. This behavior is not due to the intermolecular destacking obtained by dilution because the resulting deshielding would be canceled as observed in the AMP–monomer interaction. This implies that the dimer stacking is broken to allow the AMP complexation. Only two possibilities for a 1:1 complex are left, symbolized as follows

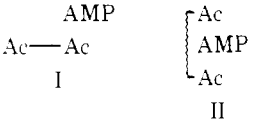

but the first structure cannot account for a large enhancement of the $\Delta\sigma_c$ nor of the K_c binding constant. Therefore, a type I complex would lead to shifts similar to those found for the AMP–acridine monomer complex. At variance, in the second model, the $\Delta\sigma_c$ must be about two times larger than in the AMP–acridine monomer complex, and such an intercalation complex is expected to be far more stable. Besides, the lower shielding current of the intercalated adenine compared with the acridine agrees with the observed downfield shift of the acridine moieties.

In this case, because the complex is made up from three stacked aromatic rings, it is not possible to propose a complex geometry. However, it is important to notice that the position of the phosphate group determines this geometry because the 3′- and 5′-AMP protons are not affected in the same ways. Equilibria in solution can be schematized in the following way:

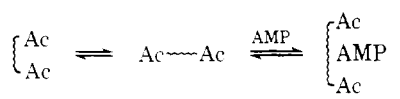

Table IV: Chemical Shift Variations ($\delta\sigma_{cex}$, ppm) of Nucleotide Protons Induced by the Complexation with the Acridine Dimer.

	Protons					
Nucleotide	$H_{1'}$ (3′)	$H_{1'}$ (5′)	H_2 (3′)	H_2 (5′)	H_8 (3′)	H_8 (5′)
3′-AMP	0.30		0.41		0.29	
5′-AMP		0.38		0.35		0.26
ApA	0.16	0.22	0.24	0.21	0.19	0.17

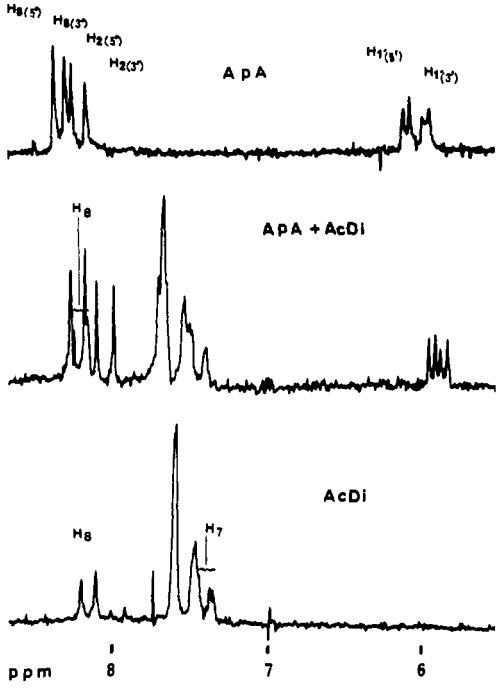

FIGURE 15: ApA–acridine dimer interaction. Concentration of ApA and AcDi is 1.2×10^{-3} M, pD 5.5, 48 °C.

(7) Study of Interactions between Acridine Dimer and ApA. Here, again, the interaction is strong. The measurements were also performed at 48 °C, pD 5.5 (Figure 15). The induced chemical shifts of the protons of the two adenine rings of ApA in the complex are reported in Table IV.

We can notice that, roughly, the shift of each proton of the complexed ApA is about one-half of the shifts of the corresponding proton in the complexed mononucleotide with AcDi. This leads us to conclude that the dinucleotide has either its 3′ or its 5′ moiety intercalated and that these two complexes are in equilibrium in about the same amount in the solution. There is no evidence for the presence of a complex of the type III.

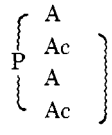

III

Here again, a geometrical description of the complexes is unrealistic. However, we can describe the state of the equilibria as follows:

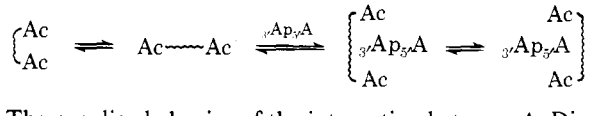

The peculiar behavior of the interaction between AcDi and ApA recalls the structure of the complex between mepacrine and ApU in mixed crystal (Seeman et al., 1975).

Conclusion

In this paper we have studied the conformation of an acridine dimer able to bis-intercalate in DNA and its interaction with AMP and ApA. These studies were performed in order to understand what are the conformational parameters and the factors which could control sequence specificity of the polyintercalation. Indeed, the eventual sequence specificity of a polyintercalating compound might probably be obtained by secondary interaction between the lateral chains of these derivatives and the bases or the sugar phosphate backbone as observed with actinomycin D (Jain and Sobell, 1972; Sobell and Jain, 1972). In these conditions the design of such a chain requires the knowledge of its allowed conformations and of the relative position of the dye and the base pairs. ^{1}H NMR spectroscopy is a powerful technique for this analysis and has demonstrated in this case that the acridine dimer interacts with a mononucleotide by intercalation of the latter between the two aromatic rings of the dye. The position of the phosphate seems to be of importance in the geometry of the complex as shown by the differences observed in the interaction of AcDi, 3′,5′-AMP, and ApA. In addition the conformation of the acridine dimer itself was analyzed and the transition between a folded $\rightleftharpoons$ unfolded structure demonstrated. This parameter is certainly very important to understand the binding to DNA because the unfolded structure is an obligatory intermediate in the intercalation process (Le Pecq et al., 1975).

Acknowledgments

The authors are grateful to Dr. B. Pullman and Dr. C. Giessner-Prettre for communication of their unpublished data on acridine ring current and to Dr. G. Hajdukovic and the Societe Cameca for recording the 250-MHz spectra.

References

Angerman, N. S., Victor, T. A., Bell, C. L., and Danyluk, S. S. (1972), *Biochemistry 11,* 2402.

Ball, E. G. (1946), *Fed. Proc. Fed. Am. Soc. Exp. Biol. 5,* 397.

Barbet, J., Roques, B. P., and Le Pecq, J. B. (1975), *C.R. Acad. Sci. (Paris) 281,* 851.

Blears, D. J., and Danyluk, S. S. (1967), *Biopolymers 5,* 535.

Brahms, J., Michelson, A. M., and Van Holde, K. E. (1966), *J. Mol. Biol. 15,* 467.

Brahms, J., and Van Holde, K. E. (1967), *Adv. Chem. Ser.* **No. 63,** 253.

Carrel, H. L. (1972), *Acta Crystallogr., Sect. B 28,* 1754.

Chan, S. I., and Nelson, J. H. (1969), *J. Am. Chem. Soc. 91,* 168.

Chan, S. I., Schweizer, M. P., Ts'o, P. O. P., and Helmkamp, G. K. (1964), *J. Am. Chem. Soc. 86,* 4182.

Courseilles, C., Barbet, J., and Hospital, M. (1976), *Acta*

Crystallogr. (in press).
Dimicoli, J. L., and Hélène, C. (1973), *J. Am. Chem. Soc. 95,* 1036.
Giessner-Prettre, C., and Pullman, B. (1970), *J. Theor. Biol. 27,* 87.
Glasoe, P. K., and Long, F. A. (1960), *J. Phys. Chem. 64,* 188.
Irvin, J. L., and Irvin, E. M. (1950), *J. Am. Chem. Soc. 72,* 2745.
Jain, S. C., and Sobell, H. M. (1972), *J. Mol. Biol. 68,* 1.
Jardetzky, C. D., and Jardetzky, O. (1960), *J. Am. Chem. Soc. 82,* 222.
Job, P. (1928), *Ann. Chim. (Paris), 9,* 113.
Kirk, J. M. (1964), *Biochim. Biophys. Acta 42,* 167.
Kreishman, G. P., Chan, S. I., and Bauer, W. (1971), *J. Mol. Biol. 61,* 45.
Krugh, T. R., and Neely, J. W. (1973), *Biochemistry 12,* 1775.
Krugh, T. R., Wittlin, F. N., and Cramer, S. P. (1975), *Biopolymers 14,* 197.
Le Pecq, J. B., Le Bret, M., Barbet, J., and Roques, B. P. (1975), *Proc. Natl. Acad. Sci. U.S.A. 72,* 2915.
Le Pecq, J. B., and Paoletti, C. (1967), *J. Mol. Biol. 27,* 87.
Lerman, L. S. (1961), *J. Mol. Biol. 3,* 18.
Lerman, L. S. (1963), *Proc. Natl. Acad. Sci. U.S.A. 49,* 94.
Lerman, L. S. (1964), *J. Cell. Comp. Physiol., Suppl. 1.,* 1.
McDonald, G., Brown, B., Hollis, D., and Walter, C. (1972), *Biochemistry 11,* 1920.
Müller, W., and Crothers, D. M. (1968), *J. Mol. Biol. 35,* 251.
Newton, B. A. (1964), in *Adv. Chemother. 1,* 35.
Patel, D. J. (1972), *Biochemistry 11,* 2388.
Robinson, B. H., Loffler, A., and Schwarz, G. (1973), *J. Chem. Soc., Faraday Trans. 1 69,* 56.
Schweitzer, M. P., Chan, S. I., and Ts'o, P. O. P. (1965), *J. Am. Chem. Soc. 87,* 5241.
Seeman, N. C., Day, R. O., and Rich, A. (1975), *Nature (London) 253,* 324.
Sobell, H. M., and Jain, S. C. (1972), *J. Mol. Biol. 68,* 21.
Thomas, G., and Roques, B. P. (1972), *FEBS Lett. 26,* 169.
Tsai, C. C., Jain, S. C., and Sobell, H. M. (1975), *Proc. Natl. Acad. Sci. U.S.A. 72,* 628.
Waring, M. J. (1965), *J. Mol. Biol. 13,* 269.

Detection of the Sites of Alkylation in DNA and Polynucleotides by Laser Raman Spectroscopy†

Samir Mansy and Warner L. Peticolas*

ABSTRACT: A laser Raman study of the alkylation of calf thymus DNA, poly(dG)·poly(dC) and poly(dA)·(dT) has been made using two water soluble alkylating agents: an antitumor drug, the difunctional methyl nitrogen mustard (HN2), which forms interstrand cross-links, and the dimethyl nitrogen half mustard (HN1). When an excess of the alkylating agent was used, the observed Raman frequencies due to the guanine ring modes in DNA and poly(dG)·poly(dC) changed virtually quantitatively to those of 7-methylguanosine (7-Me-Guo) showing that essentially all of the guanine bases were alkylated in the N-7 position. Furthermore, this alkylated DNA formed a stable double helical complex at neutral pH in which the alkylated guanine residues are in the keto form. No changes in the Raman bands of any of the other bases were observed in alkylated DNA. The DNA double helix, completely alkylated in at the N-7 position of guanine, melts about 35 °C below that of the native DNA. Upon melting, the alkylated guanine changes from the keto to the zwitterionic form.

Alkylation of nucleic acids and nucleic acid components has been of considerable interest in recent years (Michelson and Pochon, 1966; Pochon and Michelson, 1967; Ramstein et al., 1971; Engle and von Hippel, 1974; Lawley, 1966; Kohn et al., 1966). The interest in these experiments comes from the fact that nucleic acids sometimes possess alkylated bases, and alkylating agents are often either tumor-producing or tumor-inhibiting drugs. The interest in the alkylation of DNA using mustard derivatives arises from the fact that the nitrogen mustards, such as HN2,[1] *N*-methylbis(2-chloroethyl)amine hydrochloride, which are difunctional, are known to be potent tumor-inhibiting agents (Goldacre et al., 1949; Haddow et al., 1948; Loveless, 1951). Often in studies of alkylation by the difunctional alkylating agent HN2, the monofunctional alkylating agent HN1 (*N,N*-dimethyl-2-chloroethylamine hydrochloride) is also studied to obtain differences between mono- and difunctional alkylation (Kohn et al., 1966). In this paper we wish to show that alkylation of DNA and double helical polynucleotides by HN1 and HN2 leads to specific changes in their Raman spectra. From the changes in the bands it is possible to show the site of attack of the alkylating agents and the structure of the alkylated guanine residues in the DNA double helix.

Experimental Section

N,N-Dimethyl-2-chloroethylamine hydrochloride (HN1) and *N*-methylbis(2-chloroethyl)amine hydrochloride (HN2) were purchased from Aldrich Chemical Company, Milwaukee, Wisconsin. DNA calf thymus was purchased from Sigma Chemical Co., St. Louis, Missouri. The polydeoxynucleotides were purchased from Miles Laboratories, Indiana. GMP and

† From the Department of Chemistry, University of Oregon, Eugene, Oregon 97403. *Received August 15, 1975.* This work was supported in part by grants from the U.S. Public Health Service (GM 15547) and the National Science Foundation (GB-29709). Dr. Mansy holds a National Cancer Research Fellowship No. CA03254-01.

[1] Abbreviations used: HN1, *N,N*-dimethyl-2-chloroethylamine hydrochloride; HN2, *N*-methylbis(2-chloroethyl)amine hydrochloride; 7-Me-Guo, 7-methylguanosine.